NANO REACTIVE AND NONREACTIVE POLYMERS AS ASPHALT MODIFIERS FOR ANTICORROSION APPLICATION

ELSAYED M. ELNAGGAR [a]; HAZEM ELSHERIF[b]; MOHAMED A. MIGAHED [c]; AMINA M. SALEH [c]; HESHAM S. NASSAR [a] AND GAMAL M. ELKADY[a]
a Faculty of Science, Al Azhar University, Cairo, Egypt.
b National Research Centre, Cairo, Egypt.
c Egyptian Petroleum Research Institute (EPRI), Cairo, Egypt.

Abstract

Anti-corrosive coatings for carbon steel were formulated using modified asphaltic materials. Nanoparticles of polyaniline (PANI-HCl) were prepared by template free polymerization method and compared with low-density polyethylene (LDPE) as a nonreactive polymer. FT-IR proved the formation of polyaniline and XRD demonstrated a relative crystalline structure of the polymer while SEM showed fibrous nano morphology. The two types of modifiers were mixed with asphalt of type 85/25 in different percentages. SEM proved that polymer content of 4%, for both polymers, represented the most homogeneous polymer distribution in the bitumen as the continuous phase. Asphalt modification with LDPE yielded the largest values of softening point and the lowest values of penetration. The ability of modified bitumen samples, to serve as corrosion protective coatings for carbon steel, was examined by open circuit potential-time (Eocp-time) and potentiodynamic polarization in 0.5 M HCl solution. PANI-HCl based coating proved the best protective coating as it had protection efficiency of 99.997 % with corrosion rate 160.3 nm/Y.

Keywords: Nanopolymer, polyaniline, polymer-modified asphalt, anticorrosive coating.

Introduction

Asphalt is a sticky, black and highly viscous liquid or semi-solid that is present in most crude petroleums and in some natural deposits sometimes termed asphaltum**.** Asphalt is a complex mixture of aliphatic, aromatic and naphthenic hydrocarbons, with smaller quantities of other organic and metallorganic compounds. Because of the complexity of this material, the complete internal structure of asphalt is not yet known with sufficient certainty. The composition of asphalt varies with the source of the crude oil and the method of manufacturing. Asphalt is often divided into four groups according to the chemical nature (SARAs): saturates, aromatics, resins and asphaltenes. The first three groups are usually lumped together under the name maltenes. The complexity, aromaticity, heteroatom content, and molecular weight increase in the order S < A < R < As [1,2].

It is exceedingly difficult to separate individual hydrocarbon in pure form, and it is almost impossible to separate and identify all the different molecules of asphalt

[3]. Asphaltene represent the heaviest part of asphalt, with the hydrogen-carbon ratio as low as 1.15 (per mole) [4]. Thus, bitumen composition and temperature are strongly affect on the mechanical properties and microstructure of bitumen [5]. Regarding its end-use, asphalt behaves as a viscoelastic material at usual in-service temperatures, showing mechanical/rheological properties suitable for its traditional applications [6,7] that range from the construction of road pavements to more specialized purposes, such as waterproof membranes for the roofing industry [8&9].

Traditionally, the performance of bitumen has been improved through the utilization of additives such as virgin polymers waste polymers. The addition of different types of polymers to bitumen has been shown to improve its performance in a broad range of in-service temperatures [10].

Blending of asphalt with polymers form multiphase systems, and its properties depend on the concentration and the type of the polymer used. The effect of a polymer usually starts to be significant at concentrations 4–6%. Polymers that have been commonly used to modify bitumen include styrene–butadiene–styrene copolymer (SBS), styrene–butadiene rubber (SBR), styrene–isoprene–styrene copolymers, ethylene vinyl acetate (EVA), polyethylene (PE), ethylene–butyl acrylate and others [11–14]. Polymers are dispersed into bitumen, giving rise to a modified binder consisting of scattered areas of swollen polymer all over a bituminous continuous phase, with improved mechanical properties which attributed to the weak physical interactions between the polymer domains and the bitumen compounds. However, the above mentioned polymers usually present a very low compatibility with bitumen, and phase separation may eventually occur in the event of the blend being stored at high temperature in absence of stirring [15].

Recently, reactive polymers are being considered as novel bitumen modifiers, aimed to improve bitumen-polymer compatibility, and reducing the quantity of additives required. Reactive polymers are capable of forming chemical bonds with some bitumen molecules, improving the mechanical behavior, storage stability and temperature susceptibility of the resulting binder [16, 17–21].

Navarro and others [17] were studied the modification capability of MDI–PEG prepolymer as a reactive polymer compared with (SBS), recycled thermoplastic polymers (EVA/LDPE blends), and crumb tire rubber as non-reactive polymers. All the non-reactive polymer modified bitumen samples studied were largely unstable during storage at high temperature, while MDI–PEG modified bitumen remained

homogeneous because of the chemical reactions between -NCO groups of the reactive polymer with polar groups of bitumen compounds.

In general, blends of bitumen with polymers may thus have a number of applications and one of these applications is in protective coating. Protective coating is employed to protect steel structure from corrosion due to exposure in corrosive media, such as salts, humidity, ultraviolet radiation and other weather conditions. This coating function by providing a barrier between the surface and corrosion inducing elements. The performance of protective coatings are attributed to a good adhesion to substrate and a low permeability to ions, water, gases and other corrosive species of the service environment. The performance of protective coatings are attributed to a good adhesion to substrate and a low permeability to ions, water, gases and other corrosive species of the service environment. This manuscript aimed to use modified asphaltic materials to produce efficient anti-corrosive coating materials for carbon steel. To achieve this aim, nanoparticles of polyaniline (PANI-HCl) as a reactive polymer, using solution polymerization method, were prepared and characterized by FTIR, XRD and SEM. Low density polyethylene (LDPE), as a nonreactive polymer, was used for comparison. The two types of modifiers were mixed with asphalt of type 85/25 in different percentages as 2, 4, 6, 8& 10٪by the weight of the virgin bitumen. The modified asphalt samples were physically evaluated. The ability of modified bitumen samples to serve as corrosion protective coatings for carbon steel was examined by open circuit potential-time (Eocp-time), potentiodynamic polarization, and electrochemical impedance spectroscopy (EIS) measurements. The evaluation proved that the bitumen modified by PANI-HCl has higher efficacy than the bitumen modified by LDPE.

Experimental

2.1. Materials

Blown asphalt of type 85/25 was obtained from Suez For Petroleum Co. and having characteristics as illustrated in Table 1.

Table 1: Some physico-chemical characteristics of the bitumen studied

Test	ASTM standard	Value
Penetration (@25°C,100g,5s) 0.1mm	D5	25
Asphaltene content (wt. %)	D3279	30
R&B softening temperature (°C)	D36	85
Ductility at 25°C (cm)	D133	14

Two different types of polymers have been used as modifying agents: the first one was LDPE (Melt flow index (MFI) = 1.2 g/10 min, density = 0.921 kg/m^3, T_m = 110°C) and the second one was laboratory synthesized polyaniline-HCl nanoparticles. Aniline (ANI) monomer was purchased from Merck Co. and was distilled under reduced pressure prior to use. Ammonium peroxodisulfate of AR grade was purchased from Merck Co. All other chemicals were analytical grade and were used as received.

2.2. Synthesis of polyaniline

Polyaniline was prepared by the template free method [22–25]. Polyaniline was prepared by mixing (2.5 mm) aniline, dissolved in 50 ml (1M) HCl, and 20 ml aqueous solution of (1.23 mm) ammonium peroxodisulfate at 0°C to 5°C. The reaction mixture was stirred for 1hour during which aniline polymerization started. The polymerization was allowed to continue overnight, keeping the PANI suspension undisturbed. Polyaniline was created in the form of both a precipitate and a film that covered the walls of the reaction container. The polymer precipitate was separated by filtration and then rinsed with distilled water, diluted HCl and acetone to remove any residues of the monomer or oxidant. The individual stages of this process were accompanied by the well-known color changes. The so prepared PANI hydrochloride (hereinafter referred to as 'PANI-HCl') was dried in air and then at 60°C in an oven.

2.3. Characterization of the synthesized polyaniline

The FT-IR absorption spectra of the PANI samples were recorded using a "Pruker Spectrometer"; Model "Vector 22"; in Micro Analytical Center – Cairo University. Particle size and morphology of the prepared PANI were evaluated by scanning electron microscopy using SEM model quanta FEG attached with EDX Unit, with accelerating voltage 30 K.V., magnification 250x up to 1000000x and resolution for Gun.1m. The crystallinity of the prepared PANI was determined by conventional powder X-ray diffraction (XRD) using a Philips diffractometer (type PW 3710). The patterns were run with Ni-filtered copper radiation (Cu Kα = 1.5404°A at 30 kV and 10 mA) with a scanning speed of $2\theta = 2.5°\ min^{-1}$.

2.4. The modified bitumen processing [17]

The asphalt was heated in an iron container. When the asphalt temperature reached 120°Cin case of reactive polymer and 170°C in case of non-reactive polymer, a low-shear mixer was dipped into the can and set to 1200 rpm. The

polymer was added gradually (about 0.5 g/min) while keeping the temperature within the range of ±5°C during the polymer addition. Polymer modifiers were added in portions of 2, 4, 6, 8 and 10%, and the processing times were (0.5, 2 hr) for reactive and non-reactive polymers, respectively. Finally, the obtained polymer modified asphalt (PMA) was split in appropriate amounts to prepare samples for characterization.

2.5. Characterization of the modified bitumen

After determining the materials properties, conventional test methods and scanning electron microscopy analysis were conducted on each of the PMA.

2.5.1. Conventional bitumen tests

The base and PMA samples were subjected to the following conventional bitumen tests; needle penetration at 25 °C, softening point and ductility.

2.5.2. Scanning electron microscopy

Scanning electron microscopy has been used to investigate the microstructure of the PMA by determining the state of dispersion of the polymer within the base bitumen as well as characterize the nature of the continuous and discontinuous phase. By far, scanning electron microscopy is the most valuable method for studying the phase morphology of polymer-modified asphalt [26], as it allows the observation of the homogeneity and the structure in the raw state [27].

The bitumen rich phase appears dark or black, whereas the polymer rich phase appears light. Samples of each PMA were prepared (for imaging purposes) by placing a drop of heated bitumen sample between microscope slides. PMA were then examined at room temperature under SEM model quanta FEG.

2.5.3. Testing of corrosion resistance properties

The anticorrosive properties of modified bitumen were examined by open circuit potential-time (E_{ocp}-time) and potentiodynamic polarization, measurements, in 0.5 M HCl solution as electrolyte. All measurements were performed on VoltaLab 80 (PGZ402 & VoltaMaster 4) Universal Electrochemical Laboratory. Carbon steel plates (20 mm × 20 mm × 2 mm) coated with the PMA samples were used as working electrode while Pt and SCE were the counter and reference electrodes respectively. The area of 1 cm^2 was used for testing. The Tafel plots measurements were carried out at sweep rate of 20 mV/s and within the potential range from –900 to –400, –700 to –300, –1200 to –300, and from –1000 to –300 mV for [carbon steel

(CS), Asphalt, Asphalt/LDPE, and Asphalt/PANI-HCl] respectively. Tafel lines extrapolation method was used for detecting Icorr, Rp (polarization resistance), corrosion rate values and protection efficiency (P_{EF}%) for the studied systems. The Corrosion rate calculated as a number of mm of iron thickness corroded per year (the Atomic mass, Valence, Density and Working electrode area are used to calculate the corrosion rate).

3- Results and discussion

3-1: Characterization of PANI particles

3.1.1. FT-IR spectra:

Figure 1 shows the FT-IR spectra of PANI-HCl. In this figure, vibration bands at 1112, 1291, 1460 and 1572 cm^{-1} are the characteristic for polyaniline. The last two bands are assigned to C=C stretching of the benzenoid and quinoid rings, respectively and the band at 1242 cm^{-1} is characteristic for PANI emeraldine salt form [28]. The peak at 3380 cm^{-1} is assigned to N-H stretching of Benzenoid ring [29]. The band at 1290 cm^{-1} is assigned to C-N stretching of the secondary amine of PANI backbone. The band at 1112 cm^{-1} can be assigned to plane bending vibration of C-H (mode of N=Q=N, Q=N^{+}H–B and B–N^{+}H–B) which formed during protonation [30]. Therefore, the FT-IR technique confirms the PANI-HCl formation.

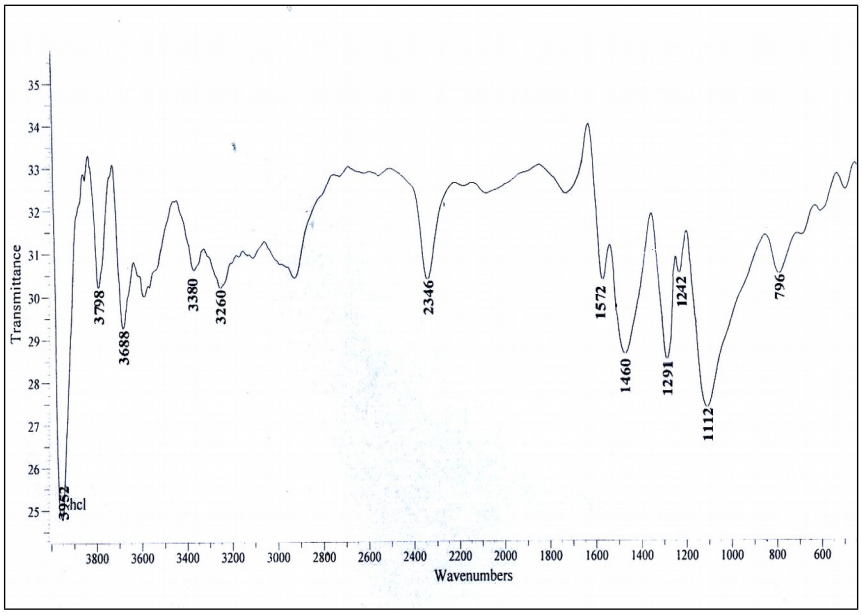

Fig 1: FT-IR Spectra for PANI-HCl

***3.1.2. Scan Electron Microscopy*:**

The aniline polymerization in acidic medium results in the formation of a protonated, partially oxidized form of PANI. This process under the test conditions leads to nano particle formation of PANI-HCl [31, 32]. Figure 2 shows SEM micrographs of the PANI-HCl nanoparticles in which particles possess almost different size distribution with fiber shapes. Diameters of the observed fibers in SEM images changes approximately from 14.57 to 500 nm, while the lengths changes approximately from 1.5 to 5μm.

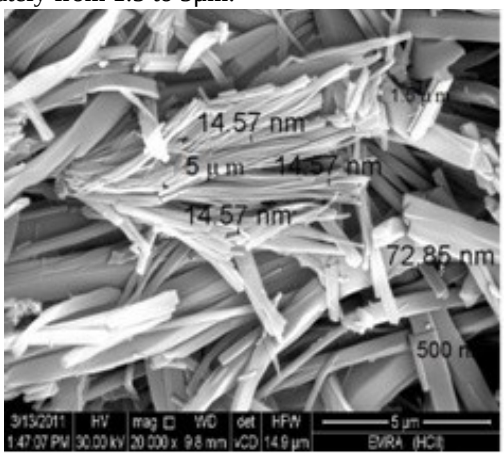

Fig 2: SEM photograph of PANI-HCl

3.1.3.X-Ray Diffraction:

X-ray diffraction is a versatile and non-destructive technique used for identification of the crystalline phases present in solid materials and for analyzing structural properties of the phases. Therefore, X-ray diffraction patterns were recorded for PANI-HCl nanopolymer (Fig. 3). The characteristic peaks were observed at 2θ = 6.445°, 19.48°, 25.80°and 26.64° This diffraction pattern also matches well with the PANI standard pattern (00-053-1890) confirming the formation of PANI-HCl nanopolymer. The intensity of the XRD pattern peaks can be influenced by crystallinity or by polyaniline chains order in polymer structure. According to Fig. 3, the alignment and the intensity of the peaks suggest that the prepared PANI-HCl has a relatively crystalline structure.

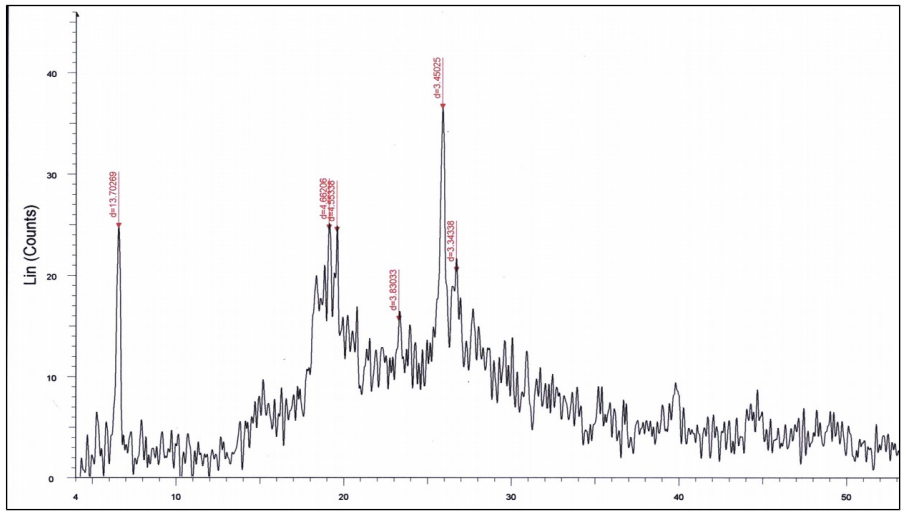

Fig. 3: X-ray diffraction patterns of PANI-HCl

3. 2: Characterization of modified bitumen

3.2.1. *Conventional tests:*

The effect of LDPE and nano PANI-HCl modification on the properties of the base bitumen can be seen in Table 2. a decrease in penetration and ductility values and an increase in softening point temperatures with the increasing polymer contents can be remarked. This trend is relatively uniform for the PANI-HCl based samples. However, there is a significant large decrease in the penetration values and a considerable increase in the softening point temperatures of LDPE based samples comparing to PMA using nonreactive polymer. The increase in softening point temperature, which is an indicator of the stiffening of PMA [33], is favorable since bitumen with higher softening point may be less susceptible to permanent deformation [34]. Polymer modification reduces temperature susceptibility (as determined by the penetration index—PI) of the bitumen. Lower values of PI indicate higher temperature susceptibility [26]. Asphalt mixtures containing bitumen with higher PI are highly resistant to low temperature cracking as well as permanent deformation at high temperature [35]. As can be seen in Table 2, all PMA samples exhibited less temperature susceptibility compared to base bitumen with the increase in the polymer content. LDPE based PMA yielded higher PI values than PANI based PMA, especially at lower polymer contents.

Table 2: Conventional properties of PMA

% Content						Property	Type
10	8	6	4	2	0		
5	6	7	8	10	25	Penetration (mm)	LDPE
150	143	138	133	123	85	Softening point(°C)	
4	6	8	9	11	14	Ductility (cm)	
5.9	5.8	5.7	5.6	5.2	3.3	Penetration index PI	
10	13	16	19	22	25	Penetration (mm)	PANI-HCl
127	118	111	104	95	85	Softening Point(°C)	
9	10	11	12	13	14	Ductility (cm)	
5.4	5.3	5.2	4.8	4.2	3.3	Penetration index PI	

SP: Softening Point.

PI = (1952−500×Log$P_{25\,°C}$−20×SP)/(50×Log$P_{25\,°C}$−SP−120)

3.2.2. Microstructure:

The microstructure of PMA samples has been investigated, using a scan electron microscope, by characterizing the nature of the continuous phase, fineness of the dispersion of the discontinuous phase as well as the description of the phases and shapes. A distinction can be made between the PMA samples whose continuous phase of a bitumen matrix and homogenous dispersed polymer particles. Scan electron microscopy images of PMA / LDPE with different ratio were shown with base bitumen in Fig. 4. In this figure, the dispersed polymer phase appears light while the bitumen phase appears dark. A clear distinction, regarding the homogeneity of the phases, is observed between the different modified samples as can be seen in Fig. 4. PMA, with the polymer content (4%), may reveal the finest homogenous dispersion of polymers and it may be deduced that increasing the polymer content could reduce the homogeneity of the PMA- LDPE.

Fig.5 shows the scan electron microscopy images of PMA / PANI-HCl with different ratio. Fortunately, PMA with the polymer content (4%) could seem to be the continuous homogenous dispersion phase for the polymer in the asphaltic matrix and the homogeneity of the PANI-HCl based PMA may be reduced by increasing the polymer content. It should be mentioned that the continuous polymer matrix, in the case of PMA with PANI-HCl, may be more compatible than LDPE based PMA with the asphaltic matrix due to polymer reactivity which may be attributed to chemical reactions between -NH groups of the reactive polymer with polar groups (-OH) of bitumen compounds.

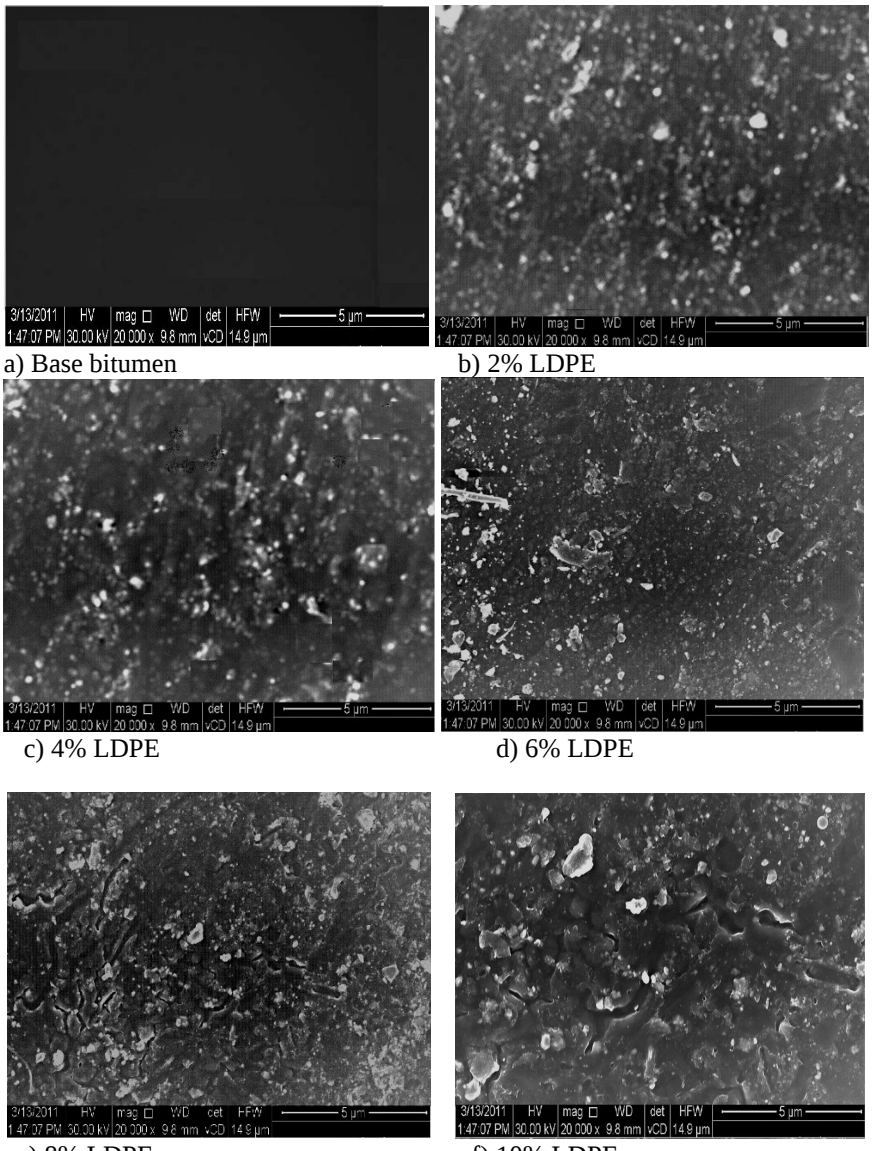

a) Base bitumen b) 2% LDPE

c) 4% LDPE d) 6% LDPE

e) 8% LDPE f) 10% LDPE

Fig. 4: SEM of PMA with LDPE

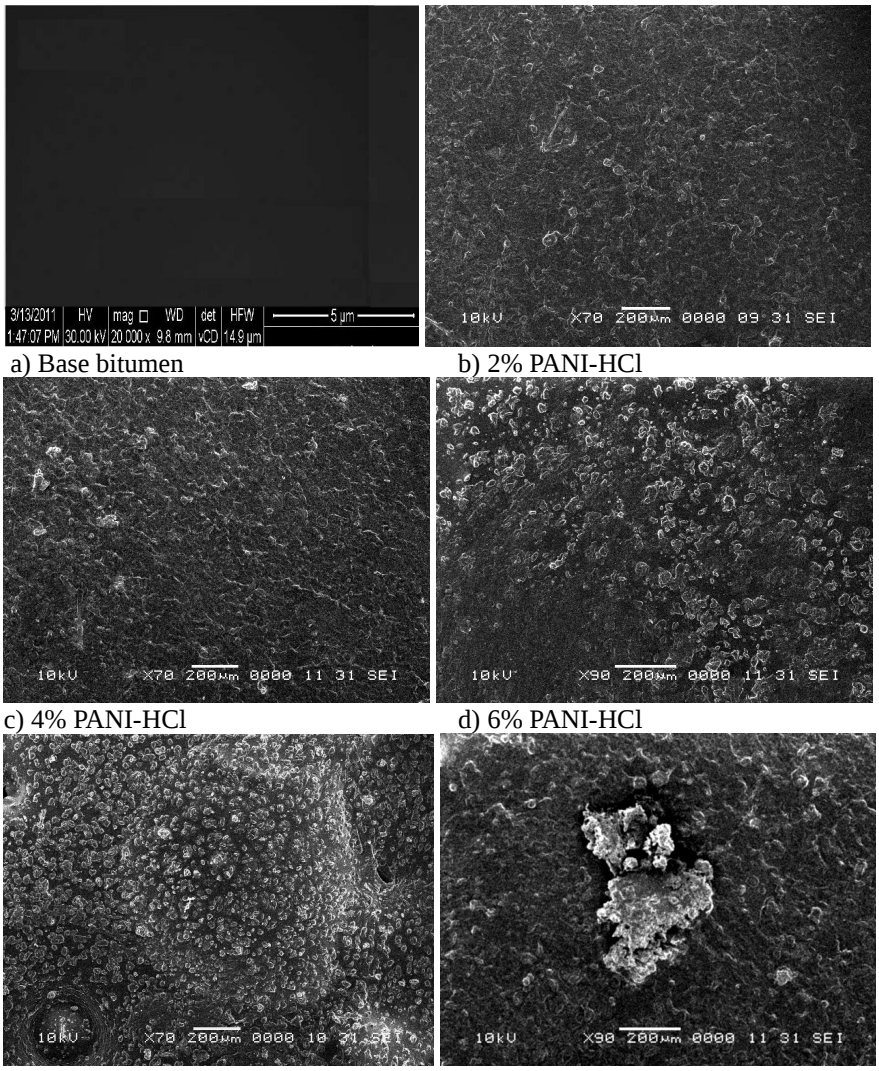

a) Base bitumen b) 2% PANI-HCl

c) 4% PANI-HCl d) 6% PANI-HCl

e) 8% PANI-HCl f) 10% PANI-HCl

Fig. 5: SEM of PMA with PANI-HCl

3. 3: Corrosion protection performance

Conducting polymer coating is used to prevent the access of corrosive environment to substrate and reduce the corrosion rate. In some cases, the redox behavior of coating generates anodic protection to substrate, and also be considered as polymeric anodic inhibitors. The degree of corrosion protection afforded by a conducting polymer coating depends on both its structural and electronic properties, which are strongly related to synthesis conditions [36].

3.3.1: Open circuit potential measurements

Potential - time curves measurements were carried out to investigate corrosion behavior of carbon steel (CS) in 0.5 M HCl in presence and absence of the modified asphaltic materials. Fig. 6 shows E_{ocp} -time curves obtained in corrosive medium, it is clear that the initial E_{ocp} value of uncoated electrode of carbon steel (CS) was -706 mV (V. SCE) and remains almost constant after 30 min of immersion time. The initial E_{ocp} of CS/Asphalt is found to be on the cathodic side of PMA samples but more positive (−530 mV) than that of CS (−706 mV), but after 30 min of exposure time to corrosive environment, the E_{ocp} shifts to more cathodic region (−640 mV). On the other hand, the coatings containing PMA have a healing effect i.e. although there is a decrease in the Eocp; it shifts to more anodic side, where the E_{ocp} value of CS/ PMA-LDPE was initially (−470 mV) and finally (−550 mV) and that of CS/PMA-PNI-HCl was initially (+2.2V) and finally (−530 mV). This tendency to shift the E_{ocp} to potentials more noble than the uncoated electrode of carbon steel is the greatest in case of PMA/PANI-HCl.

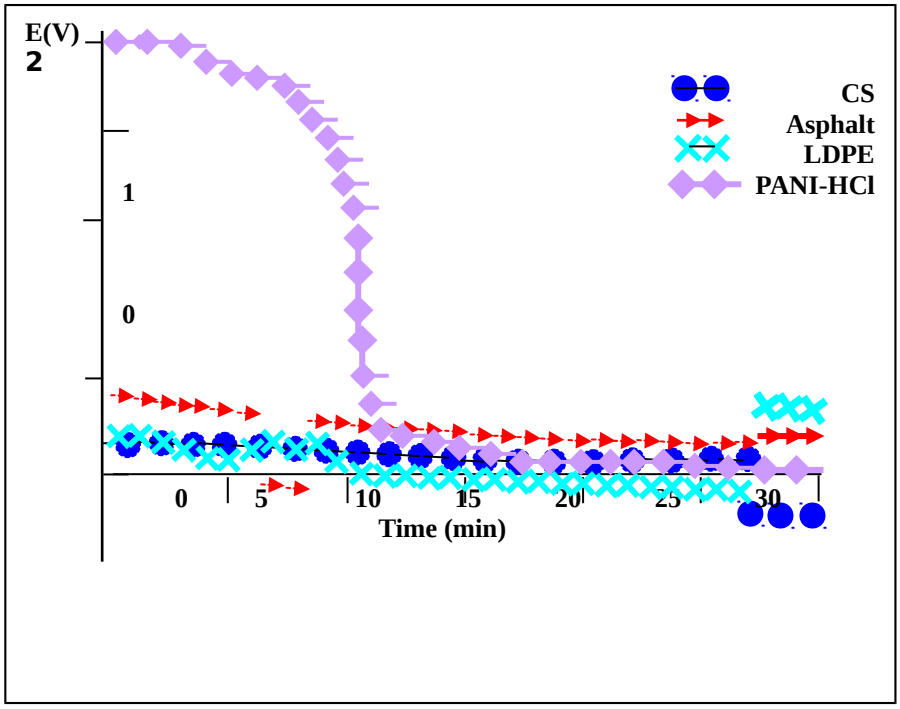

Fig. 6: E_{ocp}-time curves of uncoated CS, CS/Asphalt, CS/PMA-LDPE and CS/ PMA-PANI-HCl in 0.5M HCl

3.3.2: potentiodynamic polarization measurements

Fig. 7 shows the polarization curves for asphalt, PMA/LDPE and PMA/PANI-HCl coating on carbon steel (CS) electrodes immersed in a 0.5 M HCl. Potentiodynamic polarization is useful for compression of relative performances of various types of coatings being tested under the same conditions [37]. It is clear that the presence of coating on CS considerable reduces currents.

In fact, for PMA, the E_{ocp} remains on the anodic side of the other values even after exposure to corrosive media. The positive shift of E_{ocp} value compared to that of CS as well as asphalt coated steel clearly indicates the high corrosion resistance provided by these coatings.

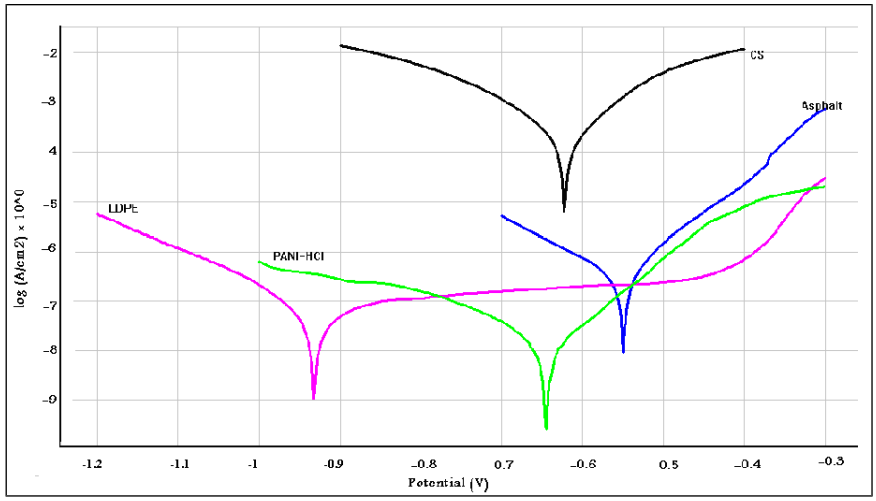

Fig. 7: Potentiodynamic polarization curves of coated and uncoated carbon steel electrodes immersed in 0.5 M HCl solution. The different types are indicated near the curves.

The corrosion parameters calculated from Tafel plots for CS, asphalt, PMA/LDPE and PMA/PANI-HCl measured were summarized in Table 2. The corrosion current, Icorr, for all three coated-electrodes are less than that observed in the uncoated CS. The lowest value of Icorr appears in case of coated CS electrode by PMA/PANI-HCl which consider the highest corrosion inhibition. However, asphalt, PMA/LDPE coated electrodes still exhibited effectively corrosion protection than the uncoated CS as identified by the corrosion current shown in Table 2.

Table 2: corrosion parameters calculated from Tafel plots

Electrode type	$I_{corr.}$	R_p	Corrosion Rate	P_{EF}%
CS	0.6447 mA/cm²	102.03 ohm.cm²	7.540 mm/Y	_
CS/asphalt	0.3111 µA/cm²	56.38 kohm.cm²	3.638 µm/Y	99.95
CS/PMA-LDPE	0.0938 µA/cm²	537.56 kohm.cm²	1.097 µm/Y	99.98
CS/PMA-PANI-HCl	0.0137 µA/cm²	1.83 Mohm.cm²	160.3 nm/Y	99.997

On the other hand, the polarization resistance, Rp, can be evaluated from the Tafel plots, according to the Stearn–Geary equation [38]:

$$R_p = b_a b_c / 2.303(b_a + b_c) I_{corr}$$

Here, Icorr is the corrosion current determined by an intersection of the linear portions of the anodic and cathodic curves, and ba and bc are the anodic and cathodic Tafel slopes ($\Delta \mathbf{E}/\Delta \log \mathbf{I}$), respectively. The protection efficiency (P_{EF}%) values were estimated using the following equation [39]:

$$P_{EF}\% = 100 \times [CR\ (uncoated) - CR\ (coated)] / CR\ (uncoated)$$

As expected, the incorporation of polymers into asphalt led to an increase of Rp value. Moreover, Rp value of PMA/PANI-HCl was the highest value. It can be remarked that the PMA/PANI-HCl coating exhibited excellent anticorrosion effect than PMA/LDPE coating. The order of the protection efficiency can be as follows: CS/asphalt<CS/asphalt PMA/LDPE <CS/asphalt PMA-PANI-HCl. This may led to the conclusion that modified bitumen with reactive polymers could greatly inhibit the steel corrosion compared with nonreactive polymers and unmodified bituminous coating. Consequently, the advantage of protection by conducting polymer coating is that the coating gets more tolerance to pin holes due to their passivation ability. The conducting polymer coating polyaniline stabilizes the potential of the metal in the passive region and maintains a protective oxide layer on the metal. It has been stated that the doped conducting polymer will generate an electric field that will restrict the flow of electrons from the metal to an outside oxidizing species thus preventing the corrosion [40]. Moreover, it is assumed that, the PANI coating protect the iron from corrosion by controlling both the anodic and cathodic reactions. The adsorption on anodic sites occurs through pi-electrons available on the conjugated aromatic ring and lone pair of electrons of nitrogen atoms, decreases anodic dissolution of iron by interacting with empty orbital of the metal. In acidic solution, the PANI acts as protonated species. These protonated species adsorb on the cathodic sites of the iron and reduce the evolution of hydrogen [41].

4- Conclusions

The chemical synthesis of reactive PANI-HCl nano-fibers were achieved by template free polymerization and characterized with FT-IR, XRD and SEM. The prepared PANI and commercial LDPE were used for modifying asphalt of penetration grade 85/25. From the resulted data, it can be concluded that a nano reactive (PANI-HCl) and nonreactive (LDPE) polymers can improve the mechanical properties of asphalt. Asphalt modification with LDPE yielded the largest values of softening point and the lowest values of penetration; which may be attributed to the oxidation of the maltene fraction during processing. On the other hand, PANI-HCl modified asphalt samples were processed at lower temperature (120°C) and during shorter processing time (30 min) than non-reactive polymer-modified asphalt, and this relatively low processing temperature avoids the significant asphalt oxidation reactions. The improvement of asphalt properties by PANI-HCl with low processing temperature is a consequence of chemical reactions between -NH groups of the reactive polymer with polar groups (-OH) of bitumen compounds. The anticorrosive properties of PMA were examined by electrochemical measurements, including Eocp-time, potentiodynamic polarization that made on coated carbon steel in 0.5 M HCl. It was found that PMA coatings are able to provide much better protection than base asphalt coatings. PANI-HCl based coating seemed to be the best one as it had protection efficiency of 99.997 % with corrosion rate of 160.3 nm/Y. The highest inhibition properties of PMA/PANI-HCl were attributed to passivation and barrier effects, while, corrosion performances of base asphalt and PMA/LDPE were related to their barrier effect.

References

1. P. Claudy, J.M. Letoffe, G.N. King, B. Brule and J.P. Planche, ; Fuel Sci. Technol. Int. 9 (1991) 71.
2. F.E. Horva´thne´ and J. Lvey, 2nd Eurasphalt & Eurobitume Congress, 1, Barcelona, Spain, 1(2000) 336–343.
3. M. Abdul Quddus; Ph.D Thesis, Department of Applied Chemistry, University of Karachi, Pakistan, (1992).
4. J. Stastna, L. Zanzotto and O.J.Vacin; J. of Colloid and Interface Sci. 259(2003) 200–207.
5. D. Lesueur, J.F. Gerard, P. Claudy, J.M. Le´ toffe´ , J.P. Planche and D. Martin; J. of Rheol. 40 (1996) 813.
6. H. Tarannum, B. Singh, M. Gupta and J. Appl.; Polym. Sci. 90 (2003) 1365.
7. A. Ait-Kadi, H. Brahimi and M. Bousmina; Polym. Eng. Sci. 36 (1996) 1724.
8. Shell-Bitumen UK. The shell bitumen handbook. Chertsey: shell Bitumen UK; 1990.
9. A.H. Fawcett and S.K. Lor; Polymer 33(1992)9, 2003–2006.
10. J.K.Newman; J. of Elast Plast, 30(1998) 245–263.
11. A. Ait-Kadi, B. Brahimi and M. Bousmina; Polym Eng Sci, 36 (1996) 12, 1724–1733.

12. R. Blanco, R. Rodriguez, M. García-Garduño and VM. Castan˜o; J. of Appl. Polym. Sci., 61(1996)9, 1493–1501.
13. S.A. Hesp and R.T. Woodhams; Colloid. Polym. Sci. 269(1991)8, 825–34.
14. A.A. Yousefi; J. of Appl. Polym. Sci. 90(2003)12, 3183–3190.
15. A. Pérez-Lepe, F. J. Martínez-Boza, P. Attane´ and C.Gallegos; J. Of Appl. Polym. Sci.,100(2006)1, 260–267.
16. H. Tarannum, B. Singh and M. Gupta; J. of Appl. Polym. Sci. 90 (2003)5, 1365-1377.
17. F.J. Navarro, P. Partal, F. Martı´nez-Boza and C. Gallegos; J. of Appl. Polym. Sci. 104(2007)3, 1683-1691.
18. G. Polacco, J. Stastna, D. Biondi, F. Antonelli, Z. Vlachovicova and L. Zanzotto; J. of Colloids Interf. Sci. 280(2004)2 366-373.
19. G. Polacco, J. Stastna, Z. Vlachovicova, D. Biondi and L. Zanzotto; Polym. Eng. Sci. 44(2004)12, 2185-2193.
20. V.Sekar, V.Selvavathi, V.Sriram and B. Sairam; J. of Pet. Sci.Technol. 20(2002)5,535-547.
21. B. Singh, H. Tarannum and M. Gupta; Constr.& Build. Mater. 18(2004)8 591-601.
22. H.J. Qiu, M.X.Wan, B. Matthews and L.M. Dai; Macromolecules 34 (2001) 675–677.
23. J. Liu and M.X. Wan; J. of Mater. Chem. 11(2001)2, 404–407.
24. Y.Z. Long, Z.J. Chen, P. Zheng, N.L. Wang, Z.M. Zhang and M.X. Wan; J. of Appl. Phys. 93(2003)5, 2962–2965.
25. Z.X. Wei and M.X. Wan; J. Appl. Polym. Sci. 87 (2003) 1297–1301.
26. A. Topal; Fuel Processing Technology, 91(2010)1, 45–51.
27. B. Brule, Y. Brion and B. Tanguy; J. of the Associ. of Asph. Pav. Tech., 57(1988)41–64.
28. M.G.Han, S.K.Cho and S.S.Im; Synth. Metals, 126 (2002)53-60.
29. V. Sridevi, S. Malathi and C.S. Devi; Chem. Sci. Jour., Volume 2011: CSJ-26.
30. A. Olad and A. Rashidzadeh; J. of Chem. Eng. 5(2008)2.
31. H. Liu, X. B. Hu, J. Y. Wang and R. I. Boughton; j. of Macromolecules, 35(2002)25, 9414-9419.
32. B.G.Soares, M.E. Leyva, G.M.O. Barra and D. Khastgir; European Polymer Journal, 42(2006)3, 676-686.
33. S. Haddadi, E. Gharbel and N. Laradi; Construction and Building Materials, 22(2008)6, 1212–1219.
34. B. Sengoz and G. Isikyakar; J. of Hazard. Mat., 150(2008)2, 424–432.
35. X. Lu and U. Isacsson; J. of Test. and Evalu., 25(1997)4, 383–390.
36. T. Tüken, B. Yazıcı and M. Erbil; Mat. Chem. and Phys. 99 (2006) (2-3),459–464.
37. E. Hur, G. Bereket and Y. Sahin; Current Appl. Phys., 7 (2007) 597–604.
38. M. Stern and AL. Geary; J. Electrochem Soc. 1957;104:56.
39. J. Bockris and KN. Reddy. Modern Electrochemistry. New York: Plenum; 1973. p. 622.
40. S. Sathiyanarayanan, S. Muthukrishnan, G. Venkatachari and D.C. Trivedi; Prog. in Org. Coat. 53 (2005) 297–301.
41. H. Bhandari, R. Srivastav, V. Choudhary and S.K. Dhawan; Thin Solid Films, 519 (2010) 1031–1039.